Published in final edited form as:

J Bone Miner Res. 2019 January ; 34(1): 171–181. doi:10.1002/jbmr.3581.

Clinically Relevant Doses of Sclerostin-Antibody do not Induce Osteonecrosis of the Jaw (ONJ) in Rats with Experimental Periodontitis

Danny Hadaya, DDS[1], **Ioannis Gkouveris, DDS, MSc, PhD**[1], **Akrivoula Soundia, DDS**[1], **Olga Bezouglaia, MS**[1], **Rogely Boyce, DVM, PhD**[2], **Marina Stolina, PhD**[3], **Denise Dwyer, BS**[3], **Sarah Dry, MD**[4], **Flavia Q Pirih, DDS, PhD**[5], **Tara L Aghaloo, DDS, MD, PhD**[1,*], and **Sotirios Tetradis, DDS, PhD**[1,*]

[1]Division of Diagnostic and Surgical Sciences, UCLA School of Dentistry, Los Angeles, CA 90095, USA.

[2]Comparative Biology and Safety Sciences, Amgen Inc., Thousand Oaks, CA, 91320

[3]Discovery Research Department, Amgen Inc., Thousand Oaks, CA, 91320

[4]Department of Pathology and Laboratory Medicine, David Geffen School of Medicine at UCLA, Los Angeles, CA 90095, USA.

[5]Division of Constitutive and Regenerative Sciences, UCLA School of Dentistry, Los Angeles, CA, 90095, USA

Abstract

Antiresorptive agents, such as bisphosphonates and denosumab, are frequently used for the management of osteoporosis. Indeed, both medications decrease the risk of osteoporotic fractures; however, these medications are associated with rare, but potentially severe side effects, such as osteonecrosis of the jaw (ONJ). ONJ, defined as an area of exposed bone in the maxillofacial region that lasts for 8 weeks, often presents with significant pain and infection, and can lead to serious complications. Interestingly, other treatments for osteoporosis have been developed, such as antibodies against the osteocyte secreted protein, sclerostin. Sclerostin functions to inhibit the Wnt signaling cascade, leading to inhibition of bone formation. In clinical trials, a sclerostin-antibody (romosozumab, Amgen Inc., UCB Brussels) increases bone formation and lowers the

[*]Corresponding Authors: Sotirios Tetradis DDS, PhD, UCLA School of Dentistry, 10833 Le Conte Ave. CHS Rm. 53-068, Los Angeles, CA 90095-1668, Tel: (310) 825-5712, Fax: (310) 825-7232 stetradis@dentistry.ucla.edu Tara L. Aghaloo DDS, MD, PhD, UCLA School of Dentistry, 10833 Le Conte Ave. CHS Rm. 53-009, Los Angeles, CA 90095-1668, Tel: (310) 794-7070, Fax: (310) 825-7232 taghaloo@dentistry.ucla. edu.

AUTHORS' ROLES

Study design: DH, RWB, TLA, and ST. Study conduct: DH, IG, AS, OB, TLA, and ST. Data analysis: DH, IG, AS, RB, MS, DD, SD, FQP, TLA, and ST. Data interpretation: DH, IG, AS, RB, MS, DD, SD, FQP, TLA, and ST. Drafting manuscript: DH, TLA, and ST. Critically revising manuscript: IG, AS, OB, RB, MS, DD, SD, and FQP. Approving final version of manuscript: DH, IG, AS, OB, RB, MS, DD, SD, FQP, TLA, and ST. All authors had full access to data and take responsibility for the integrity of the data and accuracy of the data analysis.

Disclosures

ST and TA have served as paid consultants for Amgen Inc. (Thousand Oaks, CA). ST and TA have received grant support from Amgen Inc. RB is currently a paid consultant for Amgen and MS and DD are currently Amgen employees and/or shareholders of Amgen Inc.

The other authors declare no potential conflicts of interest.

risk of osteoporotic fractures. However, in conjunction with increased osteoblastic activity, a reduction in bone resorption markers is observed. This antiresorptive effect raises the concern of possible ONJ development in patients treated with sclerostin antibodies. Here, utilizing ligature-induced experimental periodontitis (EP), we evaluated the effects of sclerostin inhibition on the development of ONJ-like lesions in ovariectomized rats. Beginning eight weeks post-ovariectomy, rats were treated for 22 weeks with weekly injections of vehicle (Veh), 200μg/kg zoledronic acid (ZA), a potent bisphosphonate at 100-fold the osteoporosis dose, or 5mg/kg sclerostin antibody (Scl-Ab) at the osteoporotic dose. EP was initiated at Week 12 and maintained for the remainder of the study. Scl-Ab treatment transiently increased serum P1NP, a bone formation marker, in serum, increased BV/TV and decreased eroded surfaces in lumbar vertebrae. ZA treated rats developed histologic features of ONJ, while Veh treated controls did not. Scl-Ab animals lost less periodontal bone in sites with EP. However, these animals presented with no histologic signs of ONJ. In conclusion, sclerostin inhibition enhanced structural bone parameters, without inducing ONJ-like lesions, in ovariectomized rats with EP.

INTRODUCTION

Osteoporosis, the most common metabolic bone disease, and osteopenia affect approximately 54% of US adults over 50 years of age, and are most common in postmenopausal women. Of this population, 20% are osteoporotic, requiring treatment, while the remaining 80% are osteopenic, for which treatment is neither currently approved, nor recommended [(1)]. Prevalence increases with age, leading to osteoporotic fractures that are associated with significant morbidity and mortality, as well as decreased mobility [(2–4)]. Management of osteoporosis largely focuses on antiresorptive agents, such as bisphosphonates (BPs), which inhibit osteoclast mediated bone resorption [(5)]. Similarly, denosumab, a monoclonal antibody against receptor activator of nuclear factor kappa-beta ligand (RANKL), inhibits osteoclast development [(6)]. Indeed, both types of medications reduce the risk of osteoporotic fractures [(7,8)]. However, treatment with antiresorptives has been associated with infrequent, but significant side effects, such as osteonecrosis of the jaw (ONJ) and atypical femoral fractures [(9)].

ONJ is an area of exposed bone in the maxillofacial region that is present for at least 8 weeks, in patients taking antiresorptive or antiangiogenic medications [(10,11)]. Although rare, ONJ can cause significant morbidity and present with pain, erythema and infection, often leading to a decrease in quality of life [(11,12)]. Described in 2003, ONJ largely occurs in the presence of anti-resorptive or anti-angiogenic therapy, in conjunction with local risk factors, such as tooth extraction and dental disease. Despite this, the molecular level disturbances surrounding ONJ have not been well characterized [(13)]. However, decreased bone resorption due to osteoclastic inhibition remains the central hypothesis in ONJ development [(10,11)].

Bone-forming agents for the treatment of osteoporosis also exist, and are analogues of parathyroid hormone (PTH), which function by directly stimulating bone formation through PTH type 1 receptors [(14–16)]. Indeed, in clinical trials, parathyroid hormone (1–34) decreased the risk of vertebral and non-vertebral fractures [(15,17)]. Despite their anabolic functions, these drugs are only recommended for a total of 24 months due to an increased

risk of osteosarcoma in rats [18]. A more recent approach towards creating anabolic interventions for the treatment of osteoporosis has been to target sclerostin, an inhibitor of bone formation, through the use of monoclonal antibodies.

Sclerostin is a secreted glycoprotein of mature osteocytes and inhibits Wnt/beta-catenin signaling, attenuating osteoblast function and differentiation [19,20]. In Phase I clinical trials, a sclerostin antibody (Scl-Ab, romosozumab, Amgen Inc., Thousand Oaks, CA & UCB Brussels, Belgium) not only showed increased bone formation markers, but also reduced levels of bone resorption markers [21]. Similarly, in Phase II and III studies, romosozumab treatment increased bone mass, reduced vertebral, non-vertebral, and hip fractures, as well as decreased bone turnover markers over the 1 year treatment period [22,23]. In another Phase III osteoporosis trial that reported reduced risk of osteoporotic fracture in the romosozumab group, two cases of ONJ were adjudicated in romosozumab treated individuals [24]. With the occurrence of ONJ in romosozumab treated osteoporotic humans, the utilization of pre-clinical animal models, known to produce ONJ-like lesions, could be helpful in improving the understanding of this adverse event.

Here, we investigated the ability of an osteoporosis treatment dose of Scl-Ab to induce ONJ-like lesions using a well-defined animal model of experimental periodontitis (EP) in ovariectomized rats. We report that similar to vehicle (Veh) treated animals, and in contrast to animals treated with zoledronic acid (ZA), a potent BP at 100x its osteoporosis treatment dose, no ONJ-like lesions were observed in rats treated with the Scl-Ab in healthy sites or sites with EP.

MATERIALS AND METHODS

Animal care

This study was approved by the UCLA Chancellor's Animal Research Committee (ARC). Animals were housed following the ARC guidelines. Rats (1 per cage) were boarded in pathogen-free conditions with a 12-hour light/dark cycle. A standard diet (NIH-31 Modified Open Formula, ENVIGO, Madison, WI, USA) and water were provided *ad libitum.* A randomized, controlled, animal model design was utilized for this prospective study, following all the recommendations of the Animal Research: Reporting In Vivo Experiments (ARRIVE) guidelines.

Experimental design (Fig. 1A)

3-month old, female Sprague Dawley rats (n=120) were purchased from Charles River Laboratories and aged to 6 months old. All animals underwent ovariectomy (OVX) at 6 months of age (average body weight at OVX=384g). After 8-weeks of bone depletion, rats were randomly assigned (n=40 per group) by body weight to receive weekly intraperitoneal (IP) injections of vehicle (Veh), 200 μg/kg ZA (LKT Laboratories, St Paul, MN), or 5 mg/kg Sclerostin-antibody, consistent with dosage provided in clinical studies [22] and designed with the same complementarity-determining region as romosozumab, but with rat Fc construct to reduce immunogenicity (Scl-AbVI, Amgen Inc., Thousand Oaks, CA & UCB Brussels, Belgium). The average body weight at the first day of Veh, ZA, or Scl-Ab

treatment was 468g. Treatment continued for 12 weeks; then, experimental periodontitis (EP), described below, was induced in the maxillae of 20/40 animals per treatment group (Veh, ZA, Scl-Ab). IP injections continued for 10 weeks, after which, animals were euthanized (Fig. 1A). The average weights at the induction of EP and necropsy were 520g and 528g, respectively. Each animal was treated as an independent unit for analysis. All investigators were blinded during allocation, experimental protocols, animal handling, and measurements. Four animals (2 Veh-EP, 1 ZA-non-EP, 1 Scl- Ab-non-EP) died following OVX due to post-operative complications.

Serum analysis

1.0 mL of blood was collected via tail vein prior to OVX, the week prior to onset of medication delivery (8 weeks post-OVX), at 6 weeks after initiation of medication delivery (14 weeks post OVX), at 12 weeks after initiation of medication delivery (20 weeks post OVX) which was the time of induced EP, and at 22 weeks after initiation of medication delivery (30 weeks post OVX). Monitoring of serum levels of procollagen type I N-terminal propeptide (P1NP) was conducted in all animals using enzyme immunoassay (Rat/Mouse P1NP EIA, IDS; Fountain Hills, AZ, USA), as described [25]. No animals treated with Scl-Ab developed P1NP levels lower than the control average during the first 12 weeks of treatment, strongly suggesting that no animals developed antidrug antibodies.

Ovariectomy

All animals underwent bilateral OVX under sterile technique. A 2-centimeter incision was made at the midline of the dorsal surface, extending from the middle of the abdominal cavity to the superior portion of the hind legs. Blunt forceps were used to dissect through the subcutaneous fat, to the muscle layer surrounding the peritoneal cavity. The incision was moved to one side, and a 1-centimeter incision was made through the muscle, over the ovary. The ovary, ovarian fat pad, and uterine horn were located, then visualized outside the peritoneal cavity. A silk suture was used to ligate the uterine horn. Following ligation, the uterine horn was severed using electrocautery. The uterine horn, ovarian fat pad, and ovary were then removed. Hemostasis was confirmed, after which the remaining uterine tissue was returned to the abdominal cavity. A resorbable 4–0 chromic suture was used to close the muscle layer. The skin incision was moved to the opposite side, and the same procedure was performed. Finally, a 4–0 non-resorbable suture was used to close the superficial incision. The superficial, non-resorbable sutures were removed under anesthesia 1 week after OVX, once wound healing was complete.

Experimental Periodontitis

EP was induced utilizing a well-established model of ligature-induced periodontitis [26–28]. All rats were anesthetized using 2% isoflurane, delivered nasally. Then, a 4–0 silk suture (FST, Foster City, CA, USA) was ligated around the left maxillary second molar (M2) in 20/40 rats per group (randomly assigned based on body weight). All animals, including non-EP animals, were briefly anesthetized once weekly, to check and replace ligatures, as necessary. One ligature, in a Veh treated animal, needed to be replaced after 4 weeks of placement.

Ex-vivo μCT specimen scanning

Dissected maxillae, and vertebrae were imaged by micro-computed tomography (SkyScan 1172; Skyscan, Kontich, Belgium) using a 20-μm isometric voxel, as described [27,29]. Bone volume fraction (BV/TV), trabecular thickness (Tb.Th), trabecular number (Tb.N), and trabecular separation (Tb.Sp) were measured using the third lumbar vertebrae. The region of interest (ROI) included the trabecular bone, 10 slices below the superior growth plate and 10 slices above the inferior growth plate of the third lumbar vertebrae. The terminology and measurements used are those recommended by the American Society for Bone and Mineral Research (ASBMR) [30].

For scanned maxillae, volumetric data were converted to Digital Imaging and Communications in Medicine (DICOM) format and imported into Dolphin Imaging software (Chatsworth, CA, USA) for three-dimensional reconstructed images. The Cemento-Enamel Junction (CEJ) to Alveolar Bone Crest (ABC) distance was measured, as described [27]. The CEJ-ABC distance was measured at 4 sites, circumferentially, around the ligated 2nd molar in each animal. Bone loss was calculated by subtracting the average CEJ-ABC distance of healthy animals from the CEJ-ABC distance in each animal with EP. Since occurrence of spontaneous maxillofacial abscesses has been reported in rodents [31,32], any animals where food, hair, bedding, and debris impaction was observed clinically and coincided with radiographic changes in the absence of EP, or radiographic changes that extended to the 1st or 3rd molars beyond the ligature site, were excluded from the study; as a result, 1 maxillae in Veh-non-EP and 2 maxillae in Scl-Ab-non-EP treated animals were excluded from analysis.

20 animals per group (Veh, ZA, Scl-Ab: 10 non-EP, 10 EP) were used for vertebral endpoints, to verify sclerostin inhibition and ZA treatment. Radiographic and histologic endpoints for ONJ in the maxilla were made in 19 Veh, 19 ZA, and 17 Scl-Ab non-EP animals, and 18 Veh, 20 ZA, and 20 Scl-Ab EP animals.

Histologic processing

Maxillae were fixed for 72 hours in 10% phosphate buffered formalin (Fisher Scientific, Hampton, NH, USA), then transferred to 70% ethanol. Following μCT scanning, samples were decalcified in 14% ethylenediaminetetraacetic acid (EDTA) for 8 weeks. Samples were paraffin embedded and 5 μm coronal sections were made, then stained with H&E. The total number of osteocytic lacunae, empty osteocytic lacunae, total bone area, osteonecrotic area, and the distance from the ABC to epithelium were measured [27]. Histology and imaging was performed at the Translational Pathology Core Laboratory (TPCL, David Geffen School of Medicine). Osteoclast enumeration was carried out using tartrate-resistant acid phosphatase (TRAP) staining (387A-IKT Sigma Aldrich, St. Louis, MO, USA). Positive cells were identified as multinucleated, TRAP-positive cells on the bone surface [27].

Bone histomorphometry

Animals were injected with 10mg/kg of 12mg/1mL calcein green (Sigma-Aldrich #C0875, St. Louis, MO, USA, C0875) in 2% sodium bicarbonate (pH 7.4) subcutaneously 10 and 3 days prior to euthanasia. Euthanasia was achieved using CO2 inhalation followed by

decapitation. OVX was verified during necropsy by confirming the absence of ovarian tissue and atrophy of uterine horn. All samples were fixed, as described above, after which the 5th and 6th lumbar vertebra (L5 & L6) were isolated, trimmed, dehydrated, and embedded in methylmethacrylate. Undecalcified parasagittal 4-p.m-thick sections of the fifth lumbar vertebral body were prepared for histomorphometric measurements, as described [33]. The ROI included the trabecular bone of the secondary spongiosa, 0.5 mm from the endosteal surface. Static and dynamic parameters, were assessed utilizing the Osteomeasure bone analysis software (Osteometrics, Inc.; Decatur, GA, USA). Eroded surface, defined as the crenated or lacunar bone surface, was assessed under polarized light to more clearly reveal the eroded lamellae.

Statistics

GraphPad Prism Software was used to analyze raw data (GraphPad Software, Inc., La Jolla, CA). P1NP serum levels before and after OVX were analyzed using a student's t-test, while time related changes were analyzed using a one-way ANOVA. Measurements were analyzed using a one-way ANOVA with post-hoc testing, with statistical significance set at $p<0.05$.

RESULTS

Serum analysis of P1NP

OVX treatment significantly decreased P1NP (Fig. 1B). No statistical differences were observed between P1NP in Veh and ZA treated animals; P1NP in ZA animals remained at Veh levels through the duration of the experiment. However, Scl-Ab animals demonstrated significantly higher levels of P1NP than Veh and ZA animals at week 6 and week 12 (Fig. 1C). P1NP in Veh animals significantly declined at 6 weeks and 22 weeks of treatment (Fig. 1C). ZA treatment significantly decreased P1NP, but only after 22 weeks of treatment relative to Week 0 (Fig. 1C). Scl-Ab treated animals, in contrast, demonstrated a significant increase in P1NP levels at 6 weeks of treatment that remained significant at 12 weeks (Fig. 1C). At 22 weeks of treatment, P1NP in Scl-Ab animals returned to the level of Veh and ZA animals (Fig. 1C).

MicroCT and histomorphometric analysis of lumbar vertebrae

μCT assessment showed an overall increase in trabecular bone mass of animals treated with ZA or Scl-Ab compared to Veh controls (Fig. 2, A-C).

ZA and Scl-Ab treatment significantly higher BV/TV (Fig. 2D) and trabecular number (Fig. 2F) compared to Veh control. For BV/TV, the Scl-Ab induced increase was statistically higher compared to the ZA effect. Scl-Ab treatment also caused a significant increase of the trabecular thickness compared to the Veh and ZA groups (Fig. 2E). Finally, trabecular separation was significantly higher in the Veh treated animals compared to the ZA or Scl-Ab treated groups. No difference between ZA and Scl-Ab treated groups was seen (Fig. 2G).

Bone histomorphometry revealed a significant decrease in mineralizing surface (MS/BS) with ZA treatment. In contrast, Scl-Ab treatment significantly increased the MS/BS compared to both Veh and ZA treated animals (Fig. 2H). Interestingly, a small but

statistically significant increase of the eroded surface (ES/BS) was noted in ZA treated animals. In contrast, in animals treated with Scl-Ab, a statistically significant decrease in ES/BS was present compared to both Veh and ZA treated groups (Fig. 2I).

Radiographic and histologic analysis of maxillae with EP

μCT analysis of healthy maxillary teeth in all groups revealed normal alveolar bone architecture, with no signs of ridge expansion (Fig. 3, A-A2, B-B2, C-C2). Animals with non-ligated molars, regardless of treatment, displayed a similar CEJ-ABC distance (Fig. 3G). Similarly, histologic examination revealed normal epithelial, submucosal and osseous architecture (data not shown).

Analysis of animals with EP revealed differences in the alveolar bone levels around the ligated molar. Extensive bone loss circumferential of M2 to the mid-root level was noted in Veh treated animals. (Fig. 3D-D2, yellow arrows). Alveolar bone loss was not apparent in ZA treated animals with EP, as the CEJ-ABC distance remained similar to that seen in non-EP rats (Fig. 3G, H). In animals treated with the Scl-Ab, alveolar bone loss was attenuated, however, not completely abolished, as seen in ZA treated animals (Fig. 3F1, yellow arrows). Quantitative assessment of alveolar bone levels revealed a statistically significant increase in the CEJ-ABC distance in Veh animals with EP (Fig. 3G). However, a decrease in alveolar bone loss of the ZA and Scl-Ab treated animals vs. Veh animals was apparent (Fig. 3H). The difference in bone loss between ZA and the Scl-Ab treated animals did not achieve statistical significance.

Histologic analysis of Veh treated animals revealed alveolar bone loss at the buccal and palatal cortices around the area of the ligature (Fig. 4A). Epithelial rimming around the ligature was present. Inflammatory infiltrate was present in the submucosa between the basal aspect of the epithelial lining and the bone crest (Fig. 4A1, yellow arrows). Osteocytic lacunae containing osteocytes was evident in the alveolar bone (Fig. 4A1, bright green arrow). In contrast, evaluation of ZA treated animals revealed a general lack of evidence of bone resorption. In addition, epithelial rimming, not only around the ligature, but also along the surface of the alveolar bone was noted (Fig. 4B, dark green arrow). Bone exposure was evident as regions of epithelial discontinuity over the underlying alveolar bone with the presence of debris (Fig. 4, B- B1, cyan arrow). Areas of necrotic bone, characterized by empty osteocytic lacunae were present in both the buccal and palatal cortices of the alveolar bone (Fig. 4B1, black arrows). Areas of dense inflammatory infiltrate were visible adjacent to the necrotic alveolar bone, around the area of the ligation (Fig. 4B1, yellow arrow). Scl-Ab animals demonstrated epithelial rimming of the ligature, a dense submucosa with inflammatory infiltrate, and mild alveolar bone loss (Fig. 4C, yellow arrows). The presence of osteocytes within the osteocytic lacunae of the alveolar bone was noted, with absence of osteonecrotic areas or bone exposure (Fig. 4C1, bright green arrow).

Picrosirius red staining of Veh, ZA, and Scl-Ab treated animals identified alterations in collagen network organization around areas of EP. In Veh and Scl-Ab dense, well-ordered collagen fibers extended from the lamina propria into the alveolar bone (Fig. 4, A3-A4, C3-C4, purple arrows). In contrast, ZA treated animals demonstrated an absence of an organized

collagen network, especially at the crestal part of the alveolar bone, where areas of osteonecrosis were noted (Fig. 4, B3, B4, white arrows).

When histologic sections of all animals were evaluated, epithelial discontinuity and bone exposure were absent in all animals with healthy periodontium, but were present in 0/18 Veh, 12/20 ZA and 0/20 Scl-Ab treated animals at the EP site ($p<0.0001$). Quantification of histologic findings revealed a significant increase of percent empty osteocytic lacunae and percent area of osteonecrosis in ZA treated animals compared to both Veh and Scl-Ab treated animals (Fig. 5A and5B). No difference between Veh and Scl-Ab treated groups was present. The epithelium to crest distance (Fig 4A1, black line), measuring the thickness of the submucosa overlying the periodontal bone was significantly decreased in ZA treated animals, in comparison to both Veh and Scl-Ab treated animals (Fig. 5C). Finally, quantification of osteoclast number showed a statistically significant decrease in ZA treated animals compared to both Veh and Scl-Ab groups (Fig. 5D).

DISCUSSION

ONJ was first described in 2003 and 2004 in patients treated with BPs [34,35]; since then, it has also been reported in patients treated with denosumab, with the first such case occurring in 2010 [36]. Although both BPs and denosumab inhibit bone resorption, they do so through distinct pharmacologic mechanisms. BPs inhibit protein farnesylation in mature, actively resorbing osteoclasts, leading to inhibited function and apoptosis, while denosumab binds to RANKL, inhibiting differentiation of osteoclast precursors, leading to decreased osteoclast formation, and thus, function [37,38]. Despite their diverse mechanisms of action, ONJ prevalence and clinical presentation are similar in BPs and denosumab, highlighting the importance of osteoclastic inhibition in ONJ pathophysiology.

Though anti-resorptives are used as frontline therapy for osteoporosis, anabolic therapy is recommended for persons who have extremely low bone mineral density or continue to fracture on anti-resorptive treatment. PTH analogs, such as teriparatide, activate both osteoblasts and osteoclasts increase bone turnover, with an overall increase in bone mineral density and decrease in fracture incidence [14,16,39]. Romosozumab, a monoclonal antibody against the Wnt inhibitor sclerostin, has been recently introduced as an alternative anabolic agent for the treatment of osteoporosis. Different than PTH analogs, in clinical trials, Scl-Ab demonstrates a dual effect on bone, increasing bone formation and decreasing bone resorption [22]. While the anabolic effects of sclerostin inhibition are well documented and understood, the effects on osteoclastic function remain poorly explained, but data suggest this occurs downstream of Wnt signaling, a mechanism distinctly different from BPs and denosumab [40]. Given Scl-Ab's osteoclastic inhibition, the possibility of adverse effects associated with its antiresorptive function cannot be excluded. Here, we used an animal model of ONJ to examine the effects of clinically-relevant doses of Scl-Ab on alveolar bone. Veh treated animals served as the negative control, while animals treated with ZA at one hundred times greater than what is used clinically for osteoporosis, served as the positive control.

First, to confirm the effects of sclerostin inhibition, we investigated serum levels of P1NP, a marker used to assess bone formation. Serum levels in ZA and Veh animals declined through the duration of the experiment, with significance noted at 6 weeks and 22 weeks in Veh treated animals, and at 22 weeks in ZA treated animals. In Scl-Ab animals, a rapid increase in P1NP was noted, lasting for 3 months, but declined to levels just below week 0 at the end of the treatment period. This is consistent with the reported self-limiting nature of the increase in bone formation elicited by sclerostin inhibition, where bone formation peaks, and begins to fall 3 months following treatment initiation [41,42]. While the mechanism of self-regulation of bone formation and bone mass is not yet well understood, multiple negative regulatory pathways appear to function downstream of canonical Wnt signaling to regulate bone formation [40].

Lumbar spine μCT measurements revealed increased bone structural values for both ZA and Scl-Ab treatments. These observations parallel results seen in OVX rats treated with Scl-Ab, as well as non-human primates [41,43,44], and parallels increases in bone mineral density seen in Phase III clinical trials of Romosozumab [22]. To further confirm the anabolic effects of Scl-Ab treatment, we conducted histomorphometric assessment of the lumbar vertebrae. Indeed, a statistically significant increase in mineralized surface (MS/BS) was observed in the animals treated with Scl-Ab, when compared to Veh treated animals. Although P1NP levels had returned to Veh levels by 22 weeks, MS/BS indicated some sustained effects on bone formation were still present. This finding confirms published data showing that MS/BS is increased by Scl-Ab treatment in both pre-clinical and clinical studies [43]. In comparison, ZA treatment significantly decreased MS/BS, far below Veh levels, consistent with previously reported data in OVX rats and monkeys treated with BPs [45,46]. Eroded surface in ZA treated animals was slightly, but significantly, higher than the Veh control group. This seemingly contradictory observation likely represents initiated resorptive sites early in treatment, when bone turnover would be highest in OVX rats. At this high dose of ZA, the resorptive site either has a protracted life span or is aborted, with failure of mature osteoclasts to effectively resorb BP containing mineralized bone [47]. Together, these data agree with the well-established role of sclerostin inhibition in increased bone formation, and subsequent improvement in bone density.

The Scl-Ab induced bone formation was accompanied by a significant decrease in bone resorption, indicated by the attenuation of ES/BS values. These observations are consistent with published data, in various animal models. In cynomolgus monkeys, Scl-Ab treatment significantly reduces eroded surface [48]. Similarly, in two independent models of OVX, Scl-Ab treatment decreases eroded trabecular surfaces through 26 weeks of treatment [25,41]. Indeed, these findings parallel human data, where levels of the bone resorption markers, TRACP-5b and CTX, decrease [22,23]. However, the mechanism through which sclerostin inhibition affects osteoclast function remains uncertain. In one study, treatment with a Scl-Ab led to increases in osteoprotegerin (OPG). Similarly, ex-vivo reports show reduced RANKL levels following sclerostin inhibition [40,42,49]. In addition, Wnt signaling is known to regulate osteoclastogenesis [50]. Finally, Scl-Ab treatment regulates expression of genes that control osteoclastogenesis in the osteocyte, such as the RANKL/OPG ratio, CSF, and WISP1 [40,51]. In contrast, ZA animals had a statistically significant increase in eroded

surface. Indeed, this is consistent with published studies, where BP treatment leads to an increase in eroded surfaces, likely due to osteoclastic activity prior to inhibition [47].

With these findings, we proceeded to investigate the local oral environment and potential development of ONJ-like features in the maxillae of Veh, ZA, and Scl-Ab treated animals employing a well-established model of EP. We and others have shown that EP in animals treated with high-dose antiresorptives induces ONJ-like lesions in rats and mice [27,52]. Radiographic evaluation confirmed the effects of EP, seen as alveolar bone loss around the second molar of Veh treated animals. In ZA treated animals, we observed the inhibition of periodontal bone loss. Similarly, Scl-Ab treatment attenuated alveolar bone loss.

Other investigators have explored the effects of sclerostin inhibition on the regeneration of periodontal tissues after EP. Scl-Ab treatment improves indices of bone formation and enhances alveolar bone volume fraction in healthy rats or rats with ovariectomy induced osteoporosis [53,54]. Interestingly, in the above studies, Scl-Ab treatment commenced after establishment of periodontal bone loss by ligature placement. Thus, the findings from these studies focus on the effects of sclerostin inhibition on the healing capacity of the periodontal tissues after removal of the instigating factor. In contrast, here, Scl-Ab was given while the ligatures were still in place, with ongoing periodontal inflammation. Collectively, these studies point to a potential role of sclerostin inhibition in the management of patients either with active periodontitis or during the regeneration phase after removal of the inflammatory factors.

Histologically, Veh treated animals showed bone resorption and inflammatory infiltrate in areas of EP. In contrast, in ZA treated animals, the alveolar bone was not resorbed and the presence of ONJ-like lesions, characterized by osteonecrotic areas and bone exposure, were noted. These findings are consistent with previous reports where dental disease and high dose antiresorptives induce ONJ-like lesions in rodents [27,52,55,56]. Importantly, animals treated with Scl-Ab, demonstrated a comparable appearance to the Veh group with low levels of empty osteocytic lacunae, a similar thickness of submucosa reflected by the epithelial to the alveolar crest distance, a well-ordered collagen network and absence of bone exposure.

The number of osteoclasts in the ZA treated animals were significantly attenuated. In contrast, Scl-Ab and Veh treated animals had similar osteoclast numbers. This was surprising given the reported effects of sclerostin inhibition in bone resorption and osteoclast function in patients or experimental animals with osteoporosis [21–23,30,42,43,57]. However, in a setting of local inflammation in mice with rheumatoid arthritis, increased osteoclast numbers are observed in the joints of sclerostin deficient mice or mice treated with a neutralizing sclerostin antibody [58]. Thus, it appears that the effects of sclerostin inhibition on osteoclast number and function is setting and possibly skeletal site dependent. For our experiments, the microenvironment of EP appears to overcome any potential systemic inhibition of osteoclastic function by sclerostin inhibition, in contrast to ZA. The distinct pattern of osteoclastic suppression around areas of EP that is associated with ONJ development was not observed in animals treated with Scl-Ab. As we and others have reported [27,29,31,52], areas of ONJ are only observed in ZA treated rodents around teeth with

periapical or periodontal inflammation, but not around healthy teeth. The combination of osteoclastic inhibition with aggressive local inflammation appear to be key contributors to osteonecrosis, while bisphosphonates alone, without an instigating local factor, are not sufficient to induce such lesions.

While our study provides insight into the potential of a Scl-Ab to induce ONJ, we only tested the clinically relevant dose of Scl-Ab. As no supraphysiologic doses of Scl-Ab were tested, no definitive conclusions can be made about their potential to cause ONJ at high doses. While the ZA treated animals did develop ONJ, the dose used was one-hundred-fold above the dose used for osteoporosis, and was intended to serve as a positive control, to verify that our model can indeed lead to the development of ONJ-like lesions in rodents. Because the incidence of ONJ in patients on osteoporotic doses of BPs is estimated at 0.001–0.01% [(11)], few animal studies investigating the ONJ incidence with osteoporotic BP doses in animals with experimental dental disease have been performed. In one such study utilizing spontaneous periodontal disease in rice rats (Oryzomys palustris) at an osteoporotic ZA dose, no gross ONJ-like lesions were observed; however, alveolar bone osteonecrosis was observed in 5% of the animals histologically [(59)]. Furthermore, we treated our rats for 22 weeks. Although this is a relatively long treatment period compared to other ONJ studies, the possibility of ONJ development in experimental setting with longer treatment cannot be excluded.

In summary, our results supported an attenuation of the periodontal bone loss during active EP in osteoporotic rats administered the osteoporosis dose of Scl-Ab. These findings paralleled systemic bone-forming effects of sclerostin inhibition in the spine. Although sclerostin inhibition has been associated with attenuation of osteoclast function in the osteoporosis setting, this did not appear to be the case in the setting of EP, where local inflammatory signals overcome the inhibition of resorption mediated by activated Wnt signaling. Consequently, no radiographic or histologic signs of ONJ-like lesions were noted in sites with EP in animals treated with a Scl-Ab, similar to Veh animals, but in contrast to animals treated with ZA, at a dose that is one-hundred-fold above the ZA osteoporosis dose.

ACKNOWLEDGEMENTS

This work was supported by grants from Amgen Inc, and by NIH/NIDCR R01 DE019465 (ST). DH was supported by T90/R90 DE007296 and F30 DE028171. We gratefully thank the Translational Pathology Core Laboratory (TPCL) at the David Geffen School of Medicine at UCLA for all histology and digital imaging services and Dr. Qing-Tian Niu for expert bone histomorphometry evaluation.

REFERENCES

1. Wright NC, Looker AC, Saag KG, Curtis JR, Delzell ES, Randall S, et al. The recent prevalence of osteoporosis and low bone mass in the United States based on bone mineral density at the femoral neck or lumbar spine. J Bone Miner Res. 11 2014;29(11):2520–6. PMC4757905 [PubMed: 24771492]
2. Jalava T, Sarna S, Pylkkanen L, Mawer B, Kanis JA, Selby P, et al. Association between vertebral fracture and increased mortality in osteoporotic patients. J Bone Miner Res. 7 2003;18(7):1254–60. [PubMed: 12854835]
3. Khosla S, Riggs BL. Pathophysiology of age-related bone loss and osteoporosis. Endocrinol Metab Clin North Am. 12 2005;34(4):1015–30, xi. [PubMed: 16310636]

4. Colon-Emeric CS, Saag KG. Osteoporotic fractures in older adults. Best Pract Res Clin Rheumatol. 8 2006;20(4):695–706. PMC1839833 [PubMed: 16979533]
5. Rodan GA, Reszka AA. Bisphosphonate mechanism of action. Curr Mol Med. 9 2002;2(6):571–7. [PubMed: 12243249]
6. Hanley DA, Adachi JD, Bell A, Brown V. Denosumab: mechanism of action and clinical outcomes. Int J Clin Pract. 12 2012;66(12):1139–46. PMC3549483 [PubMed: 22967310]
7. Cummings SR, San Martin J, McClung MR, Siris ES, Eastell R, Reid IR, et al. Denosumab for prevention of fractures in postmenopausal women with osteoporosis. N Engl J Med. 8 20 2009;361(8):756–65. [PubMed: 19671655]
8. Watts NB, Diab DL. Long-term use of bisphosphonates in osteoporosis. J Clin Endocrinol Metab. 4 2010;95(4):1555–65. [PubMed: 20173017]
9. Kennel KA, Drake MT. Adverse effects of bisphosphonates: implications for osteoporosis management. Mayo Clin Proc. 7 2009;84(7):632–7; quiz 8 PMC2704135 [PubMed: 19567717]
10. Ruggiero SL, Dodson TB, Fantasia J, Goodday R, Aghaloo T, Mehrotra B, et al. American Association of Oral and Maxillofacial Surgeons position paper on medication- related osteonecrosis of the jaw−−2014 update. J Oral Maxillofac Surg. 10 2014;72(10):1938–56. [PubMed: 25234529]
11. Khan AA, Morrison A, Hanley DA, Felsenberg D, McCauley LK, O'Ryan F, et al. Diagnosis and management of osteonecrosis of the jaw: a systematic review and international consensus. J Bone Miner Res. 1 2015;30(1):3–23. [PubMed: 25414052]
12. Miksad RA, Lai KC, Dodson TB, Woo SB, Treister NS, Akinyemi O, et al. Quality of life implications of bisphosphonate-associated osteonecrosis of the jaw. Oncologist. 2011; 16(1): 121–32. PMC3228058 [PubMed: 21212433]
13. Aghaloo T, Hazboun R, Tetradis S. Pathophysiology of Osteonecrosis of the Jaws. Oral Maxillofac Surg Clin North Am. 11 2015;27(4):489–96. PMC4908822 [PubMed: 26412796]
14. Langub MC, Monier-Faugere MC, Qi Q, Geng Z, Koszewski NJ, Malluche HH. Parathyroid hormone/parathyroid hormone-related peptide type 1 receptor in human bone. J Bone Miner Res. 3 2001;16(3):448–56. [PubMed: 11277262]
15. Miller PD, Hattersley G, Riis BJ, Williams GC, Lau E, Russo LA, et al. Effect of Abaloparatide vs Placebo on New Vertebral Fractures in Postmenopausal Women With Osteoporosis: A Randomized Clinical Trial. JAMA. 8 16 2016;316(7):722–33.
16. Body JJ, Gaich GA, Scheele WH, Kulkarni PM, Miller PD, Peretz A, et al. A randomized double-blind trial to compare the efficacy of teriparatide [recombinant human parathyroid hormone (1–34)] with alendronate in postmenopausal women with osteoporosis. J Clin Endocrinol Metab. 10 2002;87(10):4528–35. [PubMed: 12364430]
17. Neer RM, Arnaud CD, Zanchetta JR, Prince R, Gaich GA, Reginster JY, et al. Effect of parathyroid hormone (1–34) on fractures and bone mineral density in postmenopausal women with osteoporosis. N Engl J Med. 5 10 2001;344(19):1434–41. [PubMed: 11346808]
18. Vahle JL, Long GG, Sandusky G, Westmore M, Ma YL, Sato M. Bone neoplasms in F344 rats given teriparatide [rhPTH(1–34)] are dependent on duration of treatment and dose. Toxicol Pathol. Jul-8 2004;32(4):426–38. [PubMed: 15204966]
19. Lewiecki EM. Role of sclerostin in bone and cartilage and its potential as a therapeutic target in bone diseases. Ther Adv Musculoskelet Dis. 4 2014;6(2):48–57 PMC3956136 [PubMed: 24688605]
20. Moester MJ, Papapoulos SE, Lowik CW, van Bezooijen RL. Sclerostin: current knowledge and future perspectives. Calcif Tissue Int. 8 2010;87(2):99–107. PMC2903685 [PubMed: 20473488]
21. Padhi D, Jang G, Stouch B, Fang L, Posvar E. Single-dose, placebo-controlled, randomized study of AMG 785, a sclerostin monoclonal antibody. J Bone Miner Res. 1 2011;26(1):19–26. [PubMed: 20593411]
22. Saag KG, Petersen J, Brandi ML, Karaplis AC, Lorentzon M, Thomas T, et al. Romosozumab or Alendronate for Fracture Prevention in Women with Osteoporosis. N Engl J Med. 10 12 2017;377(15):1417–27. [PubMed: 28892457]
23. McClung MR, Grauer A. Romosozumab in postmenopausal women with osteopenia. N Engl J Med. 4 24 2014;370(17):1664–5.

24. Cosman F, Crittenden DB, Adachi JD, Binkley N, Czerwinski E, Ferrari S, et al. Romosozumab Treatment in Postmenopausal Women with Osteoporosis. N Engl J Med. 10 20 2016;375(16): 1532–43. [PubMed: 27641143]
25. Stolina M, Dwyer D, Niu QT, Villasenor KS, Kurimoto P, Grisanti M, et al. Temporal changes in systemic and local expression of bone turnover markers during six months of sclerostin antibody administration to ovariectomized rats. Bone. 10 2014;67:305–13. [PubMed: 25093263]
26. Graves DT, Fine D, Teng YT, Van Dyke TE, Hajishengallis G. The use of rodent models to investigate host-bacteria interactions related to periodontal diseases. J Clin Periodontol. 2 2008;35(2):89–105. PMC2649707 [PubMed: 18199146]
27. Aghaloo TL, Kang B, Sung EC, Shoff M, Ronconi M, Gotcher JE, et al. Periodontal disease and bisphosphonates induce osteonecrosis of the jaws in the rat. J Bone Miner Res. 8 2011;26(8): 1871–82. PMC3596511 [PubMed: 21351151]
28. Abe T, Hajishengallis G. Optimization of the ligature-induced periodontitis model in mice. J Immunol Methods. 8 30 2013;394(1–2):49–54. PMC3707981 [PubMed: 23672778]
29. Aghaloo TL, Cheong S, Bezouglaia O, Kostenuik P, Atti E, Dry SM, et al. RANKL inhibitors induce osteonecrosis of the jaw in mice with periapical disease. J Bone Miner Res. 4 2014;29(4): 843–54. PMC4476544 [PubMed: 24115073]
30. Bouxsein ML, Boyd SK, Christiansen BA, Guldberg RE, Jepsen KJ, Muller R. Guidelines for assessment of bone microstructure in rodents using micro-computed tomography. J Bone Miner Res. 7 2010;25(7):1468–86. [PubMed: 20533309]
31. de Molon RS, Cheong S, Bezouglaia O, Dry SM, Pirih F, Cirelli JA, et al. Spontaneous osteonecrosis of the jaws in the maxilla of mice on antiresorptive treatment: a novel ONJ mouse model. Bone. 11 2014;68:11–9. PMC4476062 [PubMed: 25093262]
32. Goto A, Sonoda J, Seki Y, Taketa Y, Ohta E, Nakano K, et al. Spontaneous gingivitis related to hair penetration in rats. J Toxicol Pathol. 9 2012;25(3):229–32. PMC3434340 [PubMed: 22988343]
33. Li X, Ominsky MS, Warmington KS, Morony S, Gong J, Cao J, et al. Sclerostin antibody treatment increases bone formation, bone mass, and bone strength in a rat model of postmenopausal osteoporosis. J Bone Miner Res. 4 2009;24(4):578–88. [PubMed: 19049336]
34. Marx RE. Pamidronate (Aredia) and zoledronate (Zometa) induced avascular necrosis of the jaws: a growing epidemic. J Oral Maxillofac Surg. 9 2003;61(9): 1115–7. [PubMed: 12966493]
35. Ruggiero SL, Mehrotra B, Rosenberg TJ, Engroff SL. Osteonecrosis of the jaws associated with the use of bisphosphonates: a review of 63 cases. J Oral Maxillofac Surg. 5 2004;62(5):527–34. [PubMed: 15122554]
36. Aghaloo TL, Felsenfeld AL, Tetradis S. Osteonecrosis of the jaw in a patient on Denosumab. J Oral Maxillofac Surg. 5 2010;68(5):959–63. PMC2880179 [PubMed: 20149510]
37. Drake MT, Clarke BL, Khosla S. Bisphosphonates: mechanism of action and role in clinical practice. Mayo Clin Proc. 9 2008;83(9):1032–45. PMC2667901 [PubMed: 18775204]
38. Baron R, Ferrari S, Russell RG. Denosumab and bisphosphonates: different mechanisms of action and effects. Bone. 4 1 2011;48(4):677–92. [PubMed: 21145999]
39. Kroll MH. Parathyroid hormone temporal effects on bone formation and resorption. Bull Math Biol. 1 2000;62(1):163–88. [PubMed: 10824426]
40. Taylor S, Ominsky MS, Hu R, Pacheco E, He YD, Brown DL, et al. Time-dependent cellular and transcriptional changes in the osteoblast lineage associated with sclerostin antibody treatment in ovariectomized rats. Bone. 3 2016;84:148–59. [PubMed: 26721737]
41. Li X, Niu QT, Warmington KS, Asuncion FJ, Dwyer D, Grisanti M, et al. Progressive increases in bone mass and bone strength in an ovariectomized rat model of osteoporosis after 26 weeks of treatment with a sclerostin antibody. Endocrinology. 12 2014;155(12):4785–97. [PubMed: 25259718]
42. Ominsky MS, Boyce RW, Li X, Ke HZ. Effects of sclerostin antibodies in animal models of osteoporosis. Bone. 3 2017;96:63–75. [PubMed: 27789417]
43. Tian X, Jee WS, Li X, Paszty C, Ke HZ. Sclerostin antibody increases bone mass by stimulating bone formation and inhibiting bone resorption in a hindlimb-immobilization rat model. Bone. 2 2011;48(2):197–201. [PubMed: 20850580]

44. Ominsky MS, Li C, Li X, Tan HL, Lee E, Barrero M, et al. Inhibition of sclerostin by monoclonal antibody enhances bone healing and improves bone density and strength of nonfractured bones. J Bone Miner Res. 5 2011;26(5): 1012–21. [PubMed: 21542004]
45. Gasser JA, Ingold P, Venturiere A, Shen V, Green JR. Long-term protective effects of zoledronic acid on cancellous and cortical bone in the ovariectomized rat. J Bone Miner Res. 4 2008;23(4): 544–51. [PubMed: 18072878]
46. Smith SY, Recker RR, Hannan M, Muller R, Bauss F. Intermittent intravenous administration of the bisphosphonate ibandronate prevents bone loss and maintains bone strength and quality in ovariectomized cynomolgus monkeys. Bone. 1 2003;32(1):45–55. [PubMed: 12584035]
47. Kostenuik PJ, Smith SY, Samadfam R, Jolette J, Zhou L, Ominsky MS. Effects of denosumab, alendronate, or denosumab following alendronate on bone turnover, calcium homeostasis, bone mass and bone strength in ovariectomized cynomolgus monkeys. J Bone Miner Res. 4 2015;30(4): 657–69. [PubMed: 25369992]
48. Ominsky MS, Niu QT, Li C, Li X, Ke HZ. Tissue-level mechanisms responsible for the increase in bone formation and bone volume by sclerostin antibody. J Bone Miner Res. 6 2014;29(6):1424–30. [PubMed: 24967455]
49. Tu X, Delgado-Calle J, Condon KW, Maycas M, Zhang H, Carlesso N, et al. Osteocytes mediate the anabolic actions of canonical Wnt/beta-catenin signaling in bone. Proc Natl Acad Sci U S A. 2 3 2015;112(5):E478–86. PMC4321271 [PubMed: 25605937]
50. Glass DA, 2nd, Bialek P, Ahn JD, Starbuck M, Patel MS, Clevers H, et al. Canonical Wnt signaling in differentiated osteoblasts controls osteoclast differentiation. Dev Cell. 5 2005;8(5):751–64. [PubMed: 15866165]
51. Wijenayaka AR, Kogawa M, Lim HP, Bonewald LF, Findlay DM, Atkins GJ. Sclerostin stimulates osteocyte support of osteoclast activity by a RANKL-dependent pathway. PLoS One. 2011;6(10):e25900 PMC3186800 [PubMed: 21991382]
52. Aguirre JI, Akhter MP, Kimmel DB, Pingel JE, Williams A, Jorgensen M, et al. Oncologic doses of zoledronic acid induce osteonecrosis of the jaw-like lesions in rice rats (Oryzomys palustris) with periodontitis. J Bone Miner Res. 10 2012;27(10):2130–43. PMC3436957 [PubMed: 22623376]
53. Taut AD, Jin Q, Chung JH, Galindo-Moreno P, Yi ES, Sugai JV, et al. Sclerostin antibody stimulates bone regeneration after experimental periodontitis. J Bone Miner Res. 11 2013;28(11): 2347–56. [PubMed: 23712325]
54. Chen H, Xu X, Liu M, Zhang W, Ke HZ, Qin A, et al. Sclerostin antibody treatment causes greater alveolar crest height and bone mass in an ovariectomized rat model of localized periodontitis. Bone. 7 2015;76:141–8. [PubMed: 25868799]
55. Kang B, Cheong S, Chaichanasakul T, Bezouglaia O, Atti E, Dry SM, et al. Periapical disease and bisphosphonates induce osteonecrosis of the jaws in mice. J Bone Miner Res. 7 2013;28(7):1631–40. PMC3688704 [PubMed: 23426919]
56. Song M, Alshaikh A, Kim T, Kim S, Dang M, Mehrazarin S, et al. Preexisting Periapical Inflammatory Condition Exacerbates Tooth Extraction-induced Bisphosphonate-related Osteonecrosis of the Jaw Lesions in Mice. J Endod. 11 2016;42(11):1641–6. PMC5085836 [PubMed: 27637460]
57. Boyce RW, Niu QT, Ominsky MS. Kinetic reconstruction reveals time-dependent effects of romosozumab on bone formation and osteoblast function in vertebral cancellous and cortical bone in cynomolgus monkeys. Bone. 8 2017;101:77–87. [PubMed: 28428078]
58. Wehmeyer C, Frank S, Beckmann D, Bottcher M, Cromme C, Konig U, et al. Sclerostin inhibition promotes TNF-dependent inflammatory joint destruction. Sci Transl Med. 3 16 2016;8(330): 330**ra**35.**ra**
59. Messer JG, Mendieta Calle JL, Jiron JM, Castillo EJ, Van Poznak C, Bhattacharyya N, et al. Zoledronic acid increases the prevalence of medication-related osteonecrosis of the jaw in a dose dependent manner in rice rats (Oryzomys palustris) with localized periodontitis. Bone. 3 2018;108:79–88. PMC5828169 [PubMed: 29289789]

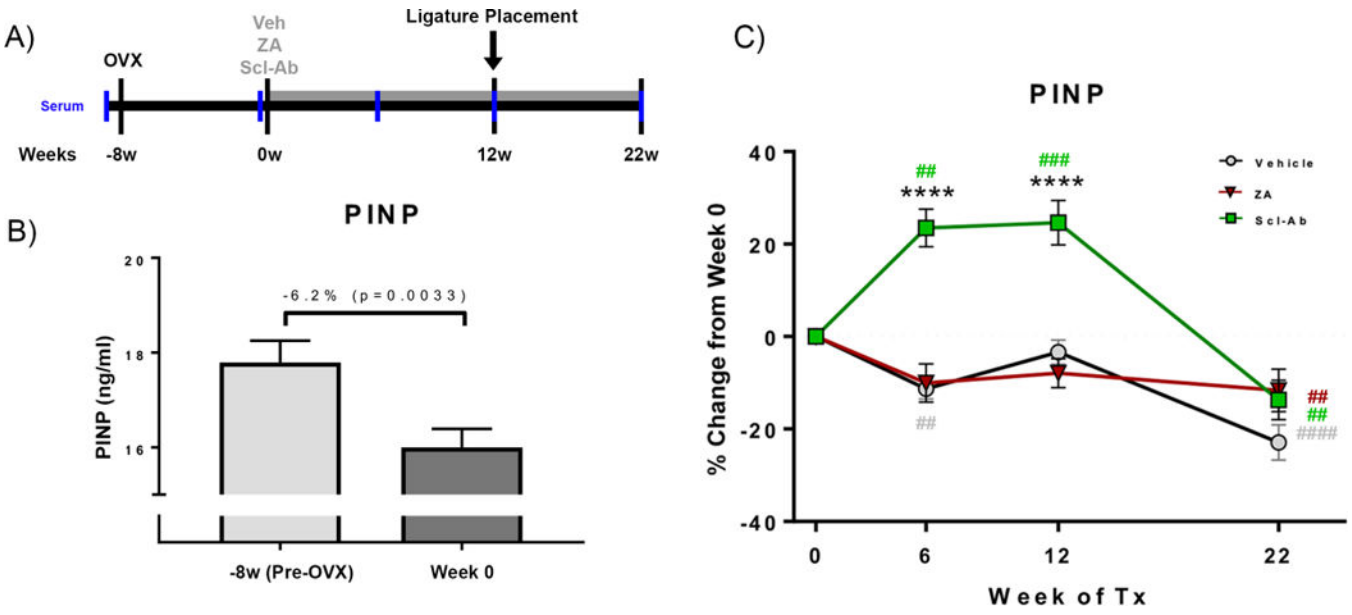

Figure 1: Experimental Timeline & Serum Analysis.

(A) Animals underwent OVX followed by an 8-week bone depletion period, after which Veh, ZA, or Scl-Ab treatment was immediately initiated. 12 weeks following treatment initiation, EP was induced. Treatment continued for 10 weeks after EP initiation, after which animals were euthanized. **(B)** Serum analysis of Pre-OVX (−8 week) and post-OVX (Week 0) P1NP. **(C)** Serum analysis of the bone formation marker, P1NP through the duration of the experiment. Data represents mean ± SEM: **** = *p<0.0001 when comparing Scl-Ab vs Veh or ZA animals. ## = p<0.01, ###= p<0.001, and #### = p<0.0001 when comparing each treatment group against Week 0 values.*

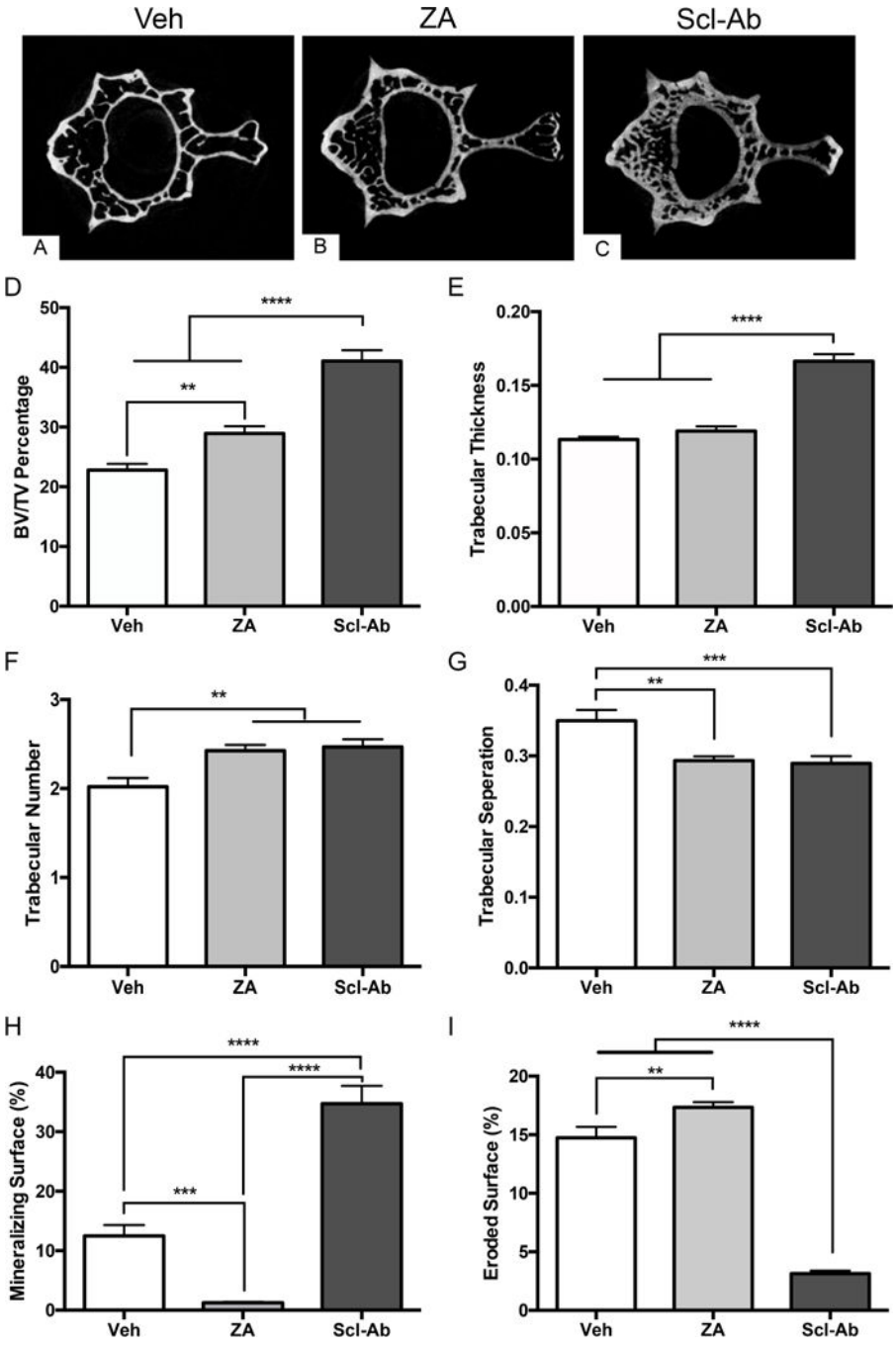

Figure 2: Radiographic Assessment of Lumbar Vertebrae.

Representative images of fourth lumbar vertebrae of **(A)** Veh, **(B)** ZA, and **(C)** Scl-Ab treated animals. **(D)** Quantification of bone volume fractionation (BV/TV). **(E)** Quantification of trabecular thickness (Tb.Th). **(F)** Quantification of trabecular number (Tb.N). **(G)** Quantification of trabecular separation (Tb.Sp). Histomorphometric quantification of **(H)** mineralized surface and **(I)** eroded surface. Data represents mean ± SEM: ****=p<0.0001, ***=p<0.001, **=p<0.01.

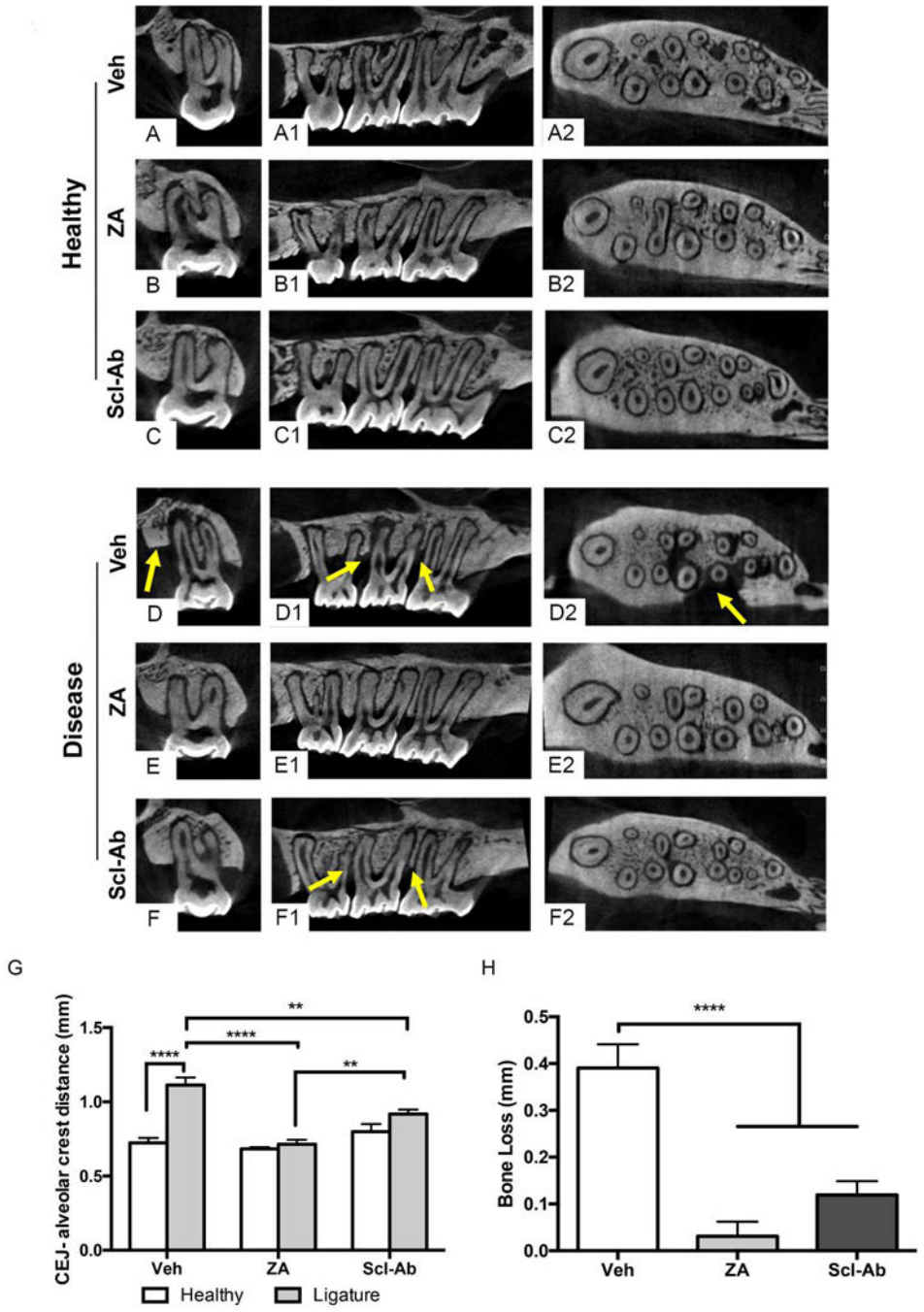

Figure 3: Radiographic Evaluation of Maxillae with EP.

Representative coronal, saggital, and axial μCT images of healthy maxillae in **(A-A2)** Veh, **(B-B2)** ZA, and **(C-C2)** Scl-Ab treated animals. Representative coronal, saggital, and axial μCT images of maxillae with EP in **(D-D2)** Veh, **(E-E2)** ZA, and **(F-F2)** Scl-Ab treated animals. Yellow arrows point to arrows of alveolar bone loss. **(G)** Quantification of CEJ-ABC distance in healthy and EP animals. **(H)** Quantification of alveolar bone loss. Data represents mean ± SEM: ****=p<0.0001, **=p<0.01.

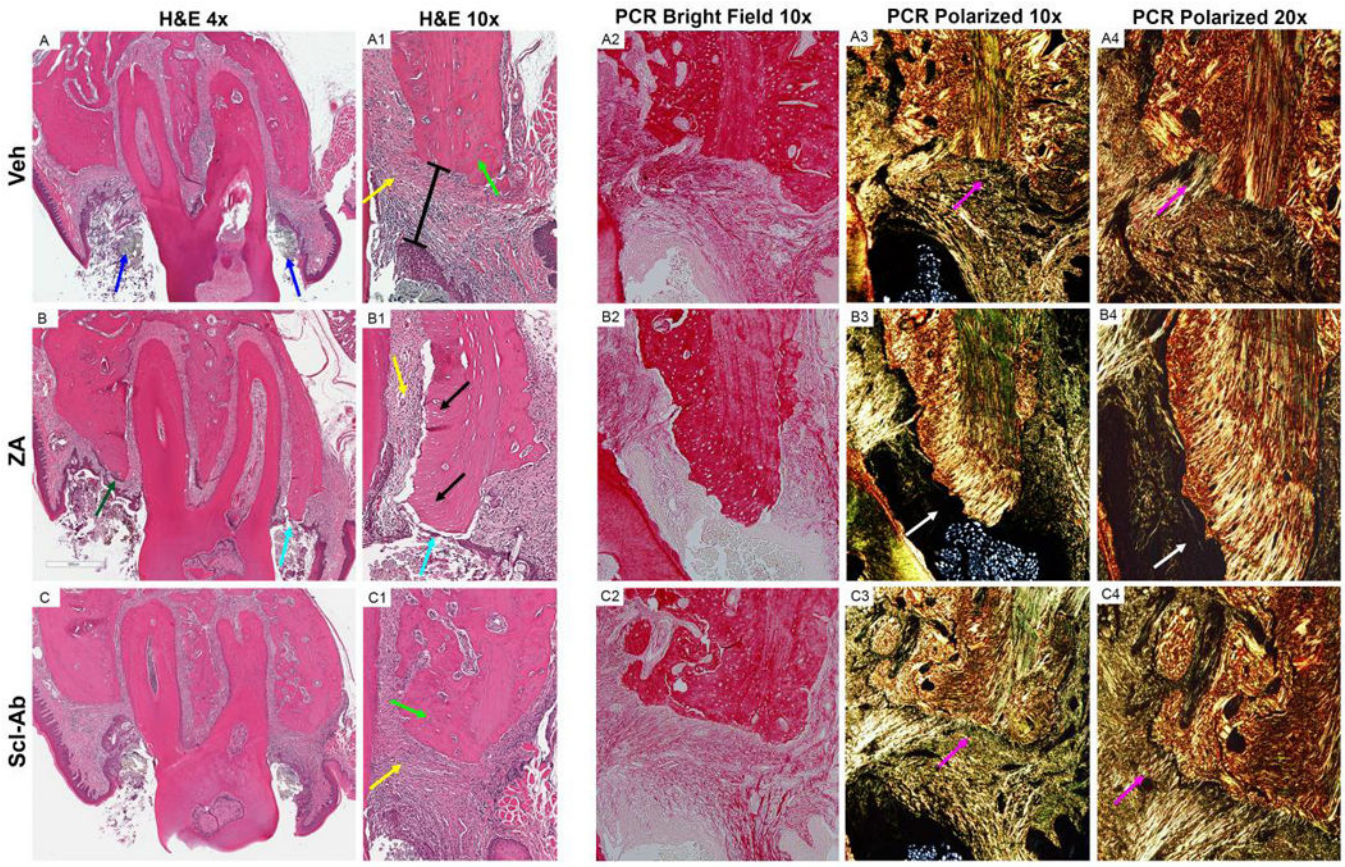

Figure 4: Histologic Analysis of Maxillae with EP

Representative coronal H&E images of maxillae with EP in **(A-A1)** Veh, **(B-B1)** ZA, and **(C- C1)** Scl-Ab treated animals. **(A)** Low power magnification of Veh treated animals with magnification of the buccal cortex shown in **(A1)**. Low magnification bright field **(A2)** and polarized images **(A3)** of Picrosirius red (PCR) staining of the palatal cortex. High powered magnification at the junction of the alveolar bone and connective tissue **(A4)**. **(B)** Low power magnification of ZA treated animals with magnification buccal cortex shown in **(B1)**. Bright field **(B2)** and polarized images of PCR staining of the palatal cortex **(B3, B4)**. **(C)** Low power magnification of Scl-Ab animals with magnification buccal cortex shown in **(C1)**. **(C2)** Bright field and **(C3, C4)** polarized images of PCR staining of the palatal cortex. Blue arrows point to the ligature. Yellow arrows point to areas of inflammatory infiltrate. Green arrows point to osteocytes within osteocytic lacunae. The black bar represents the epithelial to alveolar bone crest distance. Purple arrows point to the attachment of collagen fibers to the alveolar bone. Cyan arrows point to area of bone exposure. Black arrows points to empty osteocytic lacunae. White arrows point to an area void of collagen, adjacent to an area of osteonecrosis.

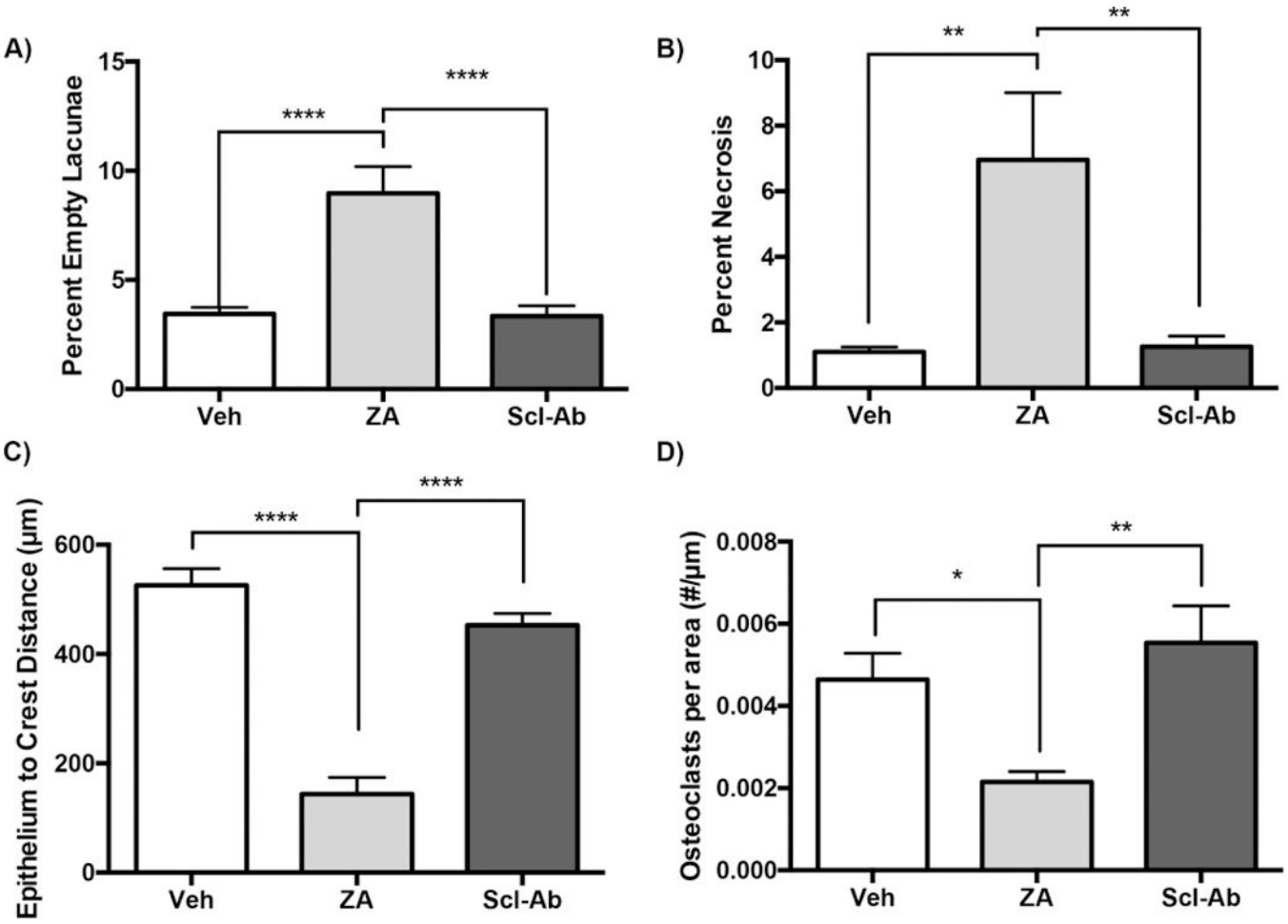

Figure 5: Quantification of Histologic Findings

Quantification of **(A)** percent empty osteocytic lacunae **(B)** percent osteonecrosis **(C)** epithelium to crest distance, and **(D)** osteoclasts per area. *Data represents mean ± SEM: ****=p<0.0001, ***=p<0.001, **=p<0.01, *=p<0.05.*